Kartografické listy / Cartographic letters, 2018, 26 (1), 10-20

VEGETATION MODELLING IN 2.5D VISIBILITY ANALYSIS

Alexandra RÁŠOVÁ

Vegetation modelling in 2.5D visibility analysis

Abstract: The effect of vegetation, so-called 'tree factor', is an issue that is often overlooked or not considered in visibility analysis. Partially, this is due to the lack of data that would express its changing characteristics, such as height, spatial extent or other properties. In this paper, we explore the possibilities of including the vegetation in the visibility analyses that relies on 2.5D digital elevation models. We discuss the modelling of stand-alone trees placed in a short distance from the viewing point, where they do not necessarily block the entire view. In the long-distance scenario, we explore the modelling techniques of opaque vegetation with known and unknown spatial extent and height. The probable viewshed proved to be a useful tool to estimate the uncertainty of the viewshed derived from global digital elevation models, which are affected by the vegetation present in these models. The proposed techniques are based on the common 2.5D modelling, so they are easy to integrate with other analytical layers.

Keywords: viewshed, visibility, vegetation, probable viewshed, spatial analysis, visual permeability, GIS, TanDEM-X, SRTM, ALOS PALSAR

Introduction

The visibility analysis is based on determination of areas that are visible from an observing point. In most GIS software packages, the basic computation is rather simple, requiring only a digital elevation model (DEM) and location of the observer position. The result is the classification of the DEM cells into visible and invisible ones. However, there are several issues that should be considered in order to achieve correct and reliable results. Connoly and Lake (2006) categorize them into computational, experimental and substantive.

The computational and experimental issues are related to the algorithm and the design of the analysis (appropriate resolution of the DEM, size of the computational area, etc.), while the substantive issues reflect various aspects of the real-life environment; the vegetation, or so the called tree-factor, is one of latter. Generally, the tree-factor is difficult to include to vegetation modelling due to its properties, which can vary in time and thus are difficult to model in 2.5D. Usually, data represent the spatial extent and height of the vegetation in a specific time point and may be outdated after few years. Various parts of the tree (the trunk, the crown) and various tree types (coniferous or deciduous, trees with broad or thin crowns) may obstruct the view differently. Their effect also depends on the distance from the observer, the viewing angle and the density of the foliage. The vegetation also changes during the year seasons. To capture all these characteristics, a detailed 3D model with a number of attributes would be needed. Nowadays, these types of datasets are generally still unavailable.

This paper is based on the dissertation thesis Rášová (2018) and focuses on three cases of vegetation modelling: i) as a solid obstacle with a known spatial extent, ii) as an obstacle with a known spatial extent that is partially transparent, and iii) as a solid obstacle with an unknown spatial extent. The vegetation that blocks the view completely and has a known spatial extent can be modelled simply by adding the vegetation to the digital terrain model – in the same way as buildings or other features would be added when creating the digital surface model.

Ing. Alexandra RÁŠOVÁ, PhD., Department of Theoretical Geodesy, Slovak University of Technology in Bratislava, Radlinského 11, 810 05 Bratislava, e-mail: alexandra.rasova@gmail.com

When the vegetation is considered as a semi-transparent obstruction, we propose an approach to model the trees that stand nearby the observer and do not cover the view entirely. The vegetation with an unknown spatial extent is a common issue when using global digital surface models. In this case, the goal is to estimate the effect of vegetation, so that the factor is considered, at least to some extent.

1. Vegetation as an obstacle in visibility modelling

The visibility is mostly determined by the landscape and landscape features, their size, the distance from the observer and exposition (Felleman, 1979). The topography of the terrain is represented by DEM; most of the viewshed algorithms are designed for a raster DEM. DEM can represent either the bare terrain (digital terrain model, DTM) or the terrain with the features that are permanently located on it, such as buildings and vegetation (digital surface model, DSM).

Modelling of the vegetation depends on the accessible datasets and their quality. In Slovakia, the main data sources include the Basic database for the geographic information system (ZB*GIS*®) and the vegetation maps. Some applications, e.g. spatial archaeology, may require knowledge of the vegetation referenced to some past time period. This information can be extracted, for instance, from the maps of potential vegetation, historical maps, or from paleobotanical researches. However, as mentioned, e.g., in Connoly and Lake (2006) or Wheatley and Gillings (2000), these datasets generally lack the resolution needed.

One of the modern data collection methods that brought new possibilities to landscape and vegetation modelling is the laser scanning. In addition to a more detailed DEM, the multiple beam reflections allowed to determine the height and density of the vegetation. For instance, Murgotio et al. (2012, 2013 and 2014) explored the use of laser scanning data for vegetation modelling in visibility analysis. They combined aerial data with the terrestrial scanning at shorter distances, leading to detailed short-distance visibility models, in which single trees are modelled in 3D at a high resolution. The 3D modelling of vegetation is used mostly in urban spaces with short-distance qualitative visibility analysis, see, e.g., Yu et al. (2016), Lin et al. (2015), or Li et al. (2015). The limit of these approaches for long-distance visibility analysis is in the amount of high-resolution data that need to be processed and collected in the first place.

Pre-laser scanning approaches were introduced by Dean (1997) and Llobera (2007). Dean (1997) proposed the visual permeability method that uses triangulated irregular surfaces (TIN). Therein, the author defines the permeability coefficient as the length of the line of sight (LoS) from the viewing point to complete obstruction of the LoS by the tree coverage. In this approach, the level of visibility decreases linearly with increasing distance. Llobera (2007) expressed the probability of visibility through vegetation via the Lambert-Beer physical law. The LoS is considered to be a beam (not a geometrical curve) that is partially influenced when passing through the vegetation. As a result, only a part of it will reach the target point. The probability of LoS getting from the observing to the observed point was expressed by Llobera (2007) using an exponential function:

$$p(x) = e^{-k(x)\cdot x} \qquad (k \geq 0,\ x > 0), \tag{1}$$

where x represents the distance from the observer and $k(x)$ is the density function. The density function and its parameters need to be derived from the vegetation properties or estimated. We simplified this approach and the function that expresses the decrease of the visibility, and used it to model the effect of stand-alone trees standing nearby the observer.

2. Experiments

In our experiments, we explore the possibilities of vegetation modelling in 2.5D visibility analysis, which is using a raster DEM, where the cells have assigned an elevation. Most of the DEMs that are available today are in 2.5D and this type of modelling can be easily integrated with other analytical layers. All computations were carried out in ArcMap 10.2, using the "Viewshed" function from the Spatial Analyst toolbox for the visibility analysis.

2.1 Vegetation as an opaque obstacle with known extent

Let us assume that we have a digital terrain model (DTM) and a vegetation dataset that contains information about its height. In this case, we can simply add the vegetation and other obstructions to the DTM. The newly created DSM will be subsequently used in the visibility analysis. This is the simplest and also the most common approach (Wheatley and Gillings, 2000; Nutsford et al., 2015).

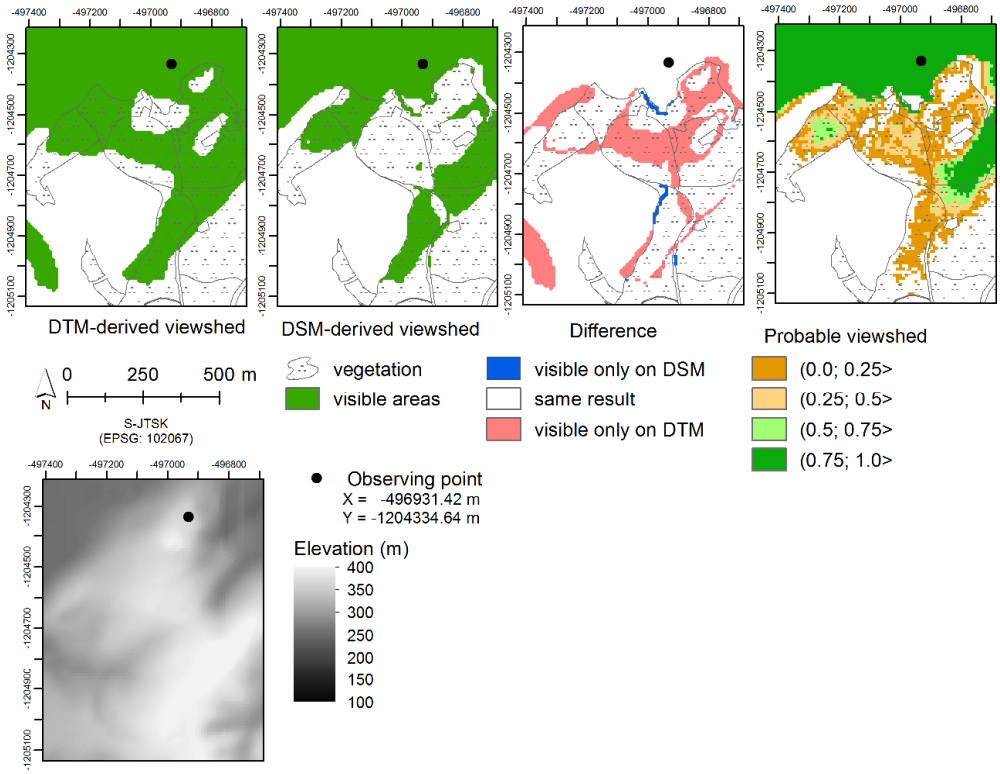

Fig. 1 Comparison of viewsheds computed using (top, from left to right) i) a digital terrain model (DTM), ii) digital surface model (DSM) that contains vegetation, iii) their difference, and iv) a probable viewshed that reflects the uncertain height of the vegetation. Terrain in the study area (shaded digital terrain model DMR-3.5, bottom)

In this experiment, we used the DTM DMR-3.5 with the resolution of 10 m that covers Slovakia. It was kindly provided to us by the Geodetic and Cartographic Institute Bratislava. The vegetation dataset was kindly provided by the National Forest Centre. In this dataset, the vegetation is represented by polygons and the vegetation heights are stored in separate attributes for the individual tree species that are located inside the polygon.

To create the DSM, the polygons were converted at first to a raster, using the height of the dominant tree species as the elevation value. In case of an unknown vegetation height, it is possible to compute the probable viewshed (Fisher, 1992). The probable viewshed estimates the probability of a cell being visible, even with small variations in the input DEM using Monte Carlo simulations. While in Rášová (2014) this method was used to consider the DEM uncertainty, here we employ it to deal with the uncertain vegetation height, using the same “Probable viewshed”

tool that was created in ModelBuilder[1]. The error component was thus added only to the grid cells covered by vegetation. From the vegetation dataset, we estimate the mean value to be 15.5 m and the standard deviation of 8.9 m. In the original dataset, the vegetation height ranges from 1 to 44 m. The probable viewshed was computed from 20 random realizations of the DSM, considering also an autocorrelation via a 3x3 smoothing filter. These settings are justified by the study of Rášová (2018), who investigated the impact of both the total number of random realizations of the DEM and the type of the smoothing filter.

In Fig.1, we compare viewsheds computed using the DTM and the DSM that was created by adding the vegetation to the DTM as well as the probable viewshed. The probable viewshed provides an estimation of the influence of the vegetation with an uncertain height. Although it does not match the DSM-derived viewshed exactly, it is possible to recognize the invisible areas (visibility value = 0), the probably visible areas (close to 1) and the uncertain areas (greater than 0, but smaller than ~1). We can see that the vegetation obstructs a portion of the view from the observing point, causing that some cells are visible only on the DSM-derived viewshed. These cells are located on the tops of tree crowns, which, thanks to their height, managed to surpass the local horizon and became visible.

We would like to stress that this is an important fact to keep in mind when designing the analysis as well as when analysing the results derived from DSMs. For instance, viewsheds are often used to analyse the reciprocal visibility. Usually, areas visible from the viewing point are considered to be also the areas, from which one can see the observing location. In this case, however, the observer of the reverse viewshed would be placed on top of the trees. Obviously, such scenario can be considered as incorrect for most practical applications. On the other hand, the reverse viewshed computation with a viewing point placed correctly on the terrain would produce viewsheds with practically no visible cells in areas covered by foliage. All cells in close vicinity of the observer would be then, say, a few meters higher than the neighbouring ones, thereby blocking the view completely. The model of visibility inside forested areas requires a different analysis design than in the open landscape, e.g. shorter observing radius or different method that will not consider the trees to be opaque blocks.

2.2 Stand-alone, partially transparent trees

Some obstacles that are present in the landscape may block the view only partially, such as the trees with their crowns obstructing a larger portion of the view than the trunks. This semi-transparency can be understood either as the permeability of the environment, or as the physical portion of the view being blocked, for instance by an obstruction covering only a part of the DEM cell in horizontal or vertical direction. The permeability of the environment can be considered in the analysis using, for instance, the exponential function (see Llobera, 2007) and the properties of the obstacle. Either way, the visibility value will decrease continuously with increasing distance from the observing point. If the obstacles block the view only partially, the visibility value will drop at the obstacle, but it will not change with the distance.

In both cases, we want to evaluate the effect of partially transparent obstacles, i.e. to determine and quantify the affected grid cells. For this experiment, artificial data were created. As the input data, we used a raster sampled at 1 m and having a constant value, thus representing a flat surface. The offset of the observer was chosen to be 1.5 m. We chose this value to simulate a height of human's eyes above the ground in a standing straight position. Five trees were placed 100 – 200 m from the observing point. Each tree was 5 m wide and 10 m tall, and had assigned a value of permeability coefficient ϕ from the interval <0;1>. Here, $\phi = 0$ means a complete obstruction of the view and $\phi = 1$ no effect on visibility.

The obstructing effect on visibility (Fig.2) was computed by a multiplication of the single viewshed raster with the raster of the total weights of the obstructions. The raster of the total weights is obtained by multiplying the individual weights of each obstruction. This means that if the LoS passes through more trees, their effects will be multiplied. The individual weight raster was computed for each tree separately and contains cells with the value 1 in areas that are not af-

[1] The tool is accessible at ArcGIS website (goo.gl/PQNAma) and its usage is described, e.g., in Rášová (2014)

fected and cells with the values of the permeability function (or the permeability coefficient of the tree) in the areas that are obstructed by the tree. In order to ensure a continuous decrease of the visibility value, we used a decreasing exponential function, where the level of the visibility drops to a half every 50 m after encountering an obstacle.

This approach is appropriate for short-distance visibility analysis, in which a larger detail is needed. In longer distances, trees appear more homogenously, stand-alone trees tend to blend with the background and larger groups of trees or forests tend to present solid, opaque obstacles.

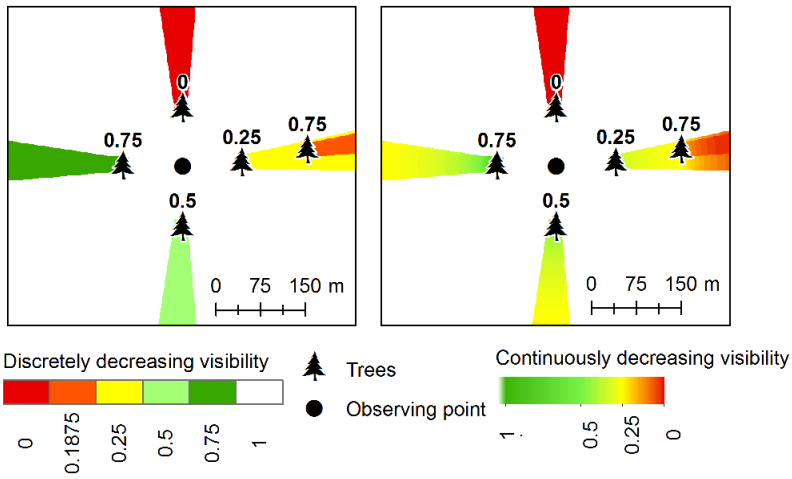

Fig. 2 Semitransparent obstacles (trees) with values of the permeability coefficient. Left: discrete decrease of visibility, right: continuous decrease of visibility using exponential function

2.3 Opaque vegetation with unknown spatial extent

Often, especially when using global DEMs that were acquired using radar interferometry, the extent of vegetation that is present after data filtering is not known. The landscape surface represented by these DEMs is not as smooth as local DEMs with higher resolution. Too often, the viewsheds derived from the global DEMs consist of scattered cells in some areas, so that it is difficult to reliably determine the visible and invisible areas.

In the next experiment, we used a study area in the northern Guatemala, which is almost completely covered by dense vegetation. The vegetation is, to some (unknown) degree, also present in the near-global DEMs (gDEMs) that we used: SRTM at the resolution of 1'' (approx. 30 m), and TanDEM-X and ALOS PALSAR, both at the resolution of 0.4'' (approx. 12 m). All three DEMs are based on radar interferometry data. A smaller part of the study area is also covered by a local DTM derived from aerial laser scanning at a much detailed resolution of 1 m (Lieskovský, Kováč a Drápela, 2017). Here, this surface is considered to be as the correct or the "true" one, due to its at least one order of magnitude better accuracy and resolution. In addition, the representation of the terrain and the viewshed derived from this surface was also considered to be the correct one.

To estimate the vegetation effect on the visibility, we computed the probable viewshed for several points using the above mentioned "Probable viewshed" tool. The probable viewshed was computed from 100 random realizations, assuming normal distribution of the error with an autocorrelation included using a 3x3 smoothening filter. The mean value and the standard deviation of the error (the error includes both the DEM error and the vegetation height) were computed from the difference between the local DEM and the gDEMs.

This process was performed for 18 observing points located on hills. Here, we demonstrate the results for two special cases (Fig. 3): i) viewing point 1, having the smallest differences between the single viewsheds, and ii) viewing point 2, where the single viewsheds from global DEMs differ

the most from the viewshed that relies on the local DEM. Here, we compare the single viewsheds computed on local DEM and single and probable viewsheds computed on gDEM. In this comparison, all cells with the probable viewshed value higher than 0 are considered to be potentially visible. It should be noted that the gDEMs have lower resolution than the local DEM derived from LiDAR, which means they are unable to capture the same level of detail. As a result, at least some portion of the discrepancies between the local DEM and gDEMs is probably caused by the different resolutions.

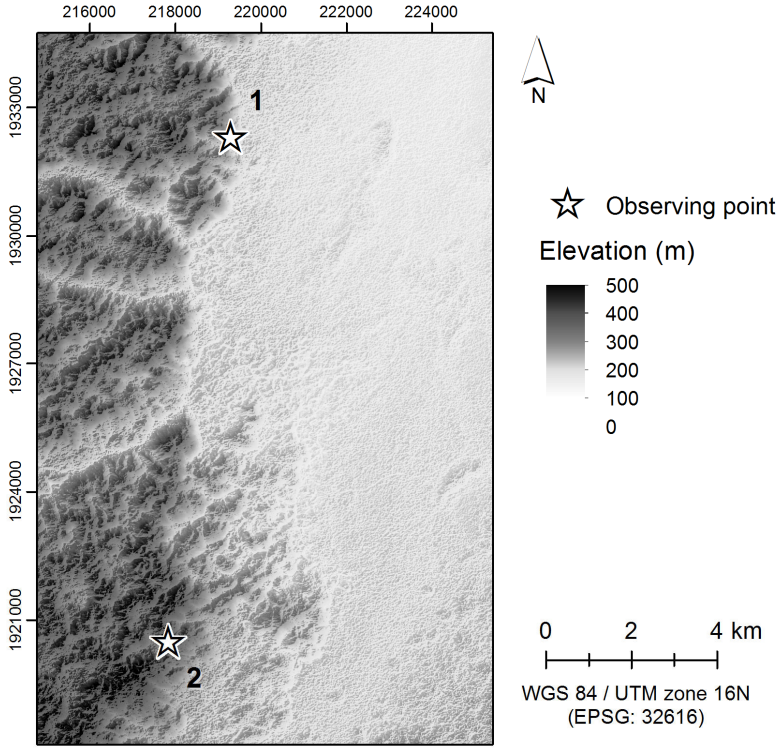

Fig. 3 Study area in northern Guatemala (shaded TanDEM-X digital elevation model)

The single viewsheds from the observing point 1 (Fig. 4, Tab.1) appear to be similar for all DEMs. It is also seen that the probable viewshed produced some sort of a buffer around the visible cells, thus representing the uncertainty of the single viewshed. Overall, there are 23-26 % of potentially visible cells that were originally invisible in the single viewshed. The majority of the potentially visible cells have values from the interval (0.0, 0.2>. The amount of cells with the probable viewshed value = 1 is less than 1 % for each gDEM, which means that there are only very few locations that are unaffected by the small changes of the terrain elevation. The comparison with the local, more accurate, DEM is reported in Tab. 3. We observe that all gDEMs have similar results in terms of agreement with the local DEM: about 82-83 % of cells were evaluated identically, being either visible or invisible on the local DEM as well as on the respective gDEM. Interestingly, some cells (2-7 %) were identified as visible only on the local more accurate DEM, which means that their probability of being visible on the probable viewshed was equal to 0. Other cells that were detected as invisible on the local DEM were potentially visible on gDEMs (11-16 %).

On the other hand, the limited views from the observing point 2 (Fig. 5, Tab.1) derived from the gDEMs are significantly enlarged by the probable viewshed, which is in accordance with the single viewshed from the local DEM. The values of probable viewshed are prevalently 0 or close

to 0 for each gDEM, with less than 0.2 % of cells having the probability of 1.0. Again, this indicates that relatively small changes of terrain between the observing point and target cell can have a large impact on the visibility. The comparison of potentially visible cells and the single viewshed computed on the local DEM are in Tab. 3. In this case, there are larger differences between the gDEMs. While 80 % of TanDEM-X cells were evaluated in accordance with the local DEM (similar percentage as for observing point 1), both ALOS PALSAR and SRTM have significantly lower agreement with the local DEM (48.4 % and 47.1 %, respectively). These two models have also higher percentage of potentially visible cells that were invisible on local DEM (ALOS PALSAR 39 %, SRTM 45.4 %) than TanDEM-X (less than 6 %). Thus, although the single viewshed from the TanDEM-X model contained the lowest amount of visible cells, the probable viewshed based on this model is closest to our reference result as can be seen from Fig. 5. This experiment therefore indicates that the probable viewshed should be preferred over its single counterpart, especially when the quality of the used DEM is low or unknown. In that case, the errors caused by the uncertain elevations in the DEM can be reduced, at least to some extent, resulting in potentially more accurate information on the visibility in that area.

Tab. 1 Comparison of area visible from the observing point 1. Single viewshed (SV) cells have values 0 (invisible) or 1 (visible). Probable viewshed (PV) cells values are in a range from 0 to 1.

DEM	Visibility													
	0.0		(0.0, 0.2>		(0.2, 0.4>		(0.4, 0.6>		(0.6, 0.8>		(0.8, 1.0)		1.0	
	%	km^2	%	km^2	%	km^2	%	km^2	%	km^2	%	km^2	%	km^2
Local DEM, SV	64.1	87.4	-	-	-	-	-	-	-	-	-	-	35.9	48.8
TanDEM-X, SV	86.4	117.7	-	-	-	-	-	-	-	-	-	-	13.6	18.5
TanDEM-X, PV	60.4	82.2	21.2	28.8	8.0	10.9	4.6	6.2	3.1	4.2	2.7	3.7	0.1	0.2
ALOS PALSAR, SV	76.8	104.6	-	-	-	-	-	-	-	-	-	-	23.2	31.6
ALOS PALSAR, PV	53.3	72.5	22.5	30.6	11.7	16.0	7.0	9.6	3.8	5.2	1.7	2.4	0.003	0.005
SRTM, SV	73.3	99.9	-	-	-	-	-	-	-	-	-	-	26.7	36.3
SRTM, PV	50.3	68.5	15.6	21.3	9.9	13.5	8.3	11.3	7.2	9.8	7.8	10.6	0.9	1.2

Tab. 2 Comparison of area visible from the observing point 2. Single viewshed (SV) cells have values 0 (invisible) or 1 (visible). Probable viewshed (PV) cells values are in a range from 0 to 1.

DEM	Visibility													
	0.0		(0.0, 0.2>		(0.2, 0.4>		(0.4, 0.6>		(0.6, 0.8>		(0.8, 1.0)		1.0	
	%	km^2	%	km^2	%	km^2	%	km^2	%	km^2	%	km^2	%	km^2
Local DEM, SV	54.3	74.0	-	-	-	-	-	-	-	-	-	-	45.7	62.2
TanDEM-X, SV	97.7	133.1	-	-	-	-	-	-	-	-	-	-	2.3	3.1
TanDEM-X, PV	63.1	85.9	33.9	46.1	1.5	2.1	0.4	0.6	0.4	0.5	0.6	0.8	0.1	0.1
ALOS PALSAR, SV	88.7	120.8	-	-	-	-	-	-	-	-	-	-	11.3	15.4
ALOS PALSAR, PV	61.0	83.0	33.7	45.8	4.2	5.7	0.4	0.5	0.3	0.5	0.4	0.6	0.04	0.1
SRTM, SV	87.7	119.4	-	-	-	-	-	-	-	-	-	-	12.3	16.8
SRTM, PV	54.5	74.3	27.6	37.6	10.5	14.4	5.0	6.8	1.5	2.1	0.6	0.9	0.2	0.3

Tab. 3 Differences between the probable viewsheds and reference single viewshed derived from local LiDAR-based DEM. All cells with the probable viewshed value > 0 are considered to be potentially visible.

	Agreement with the local DEM		Potentially visible only on the local DEM		Potentially visible only on the gDEM	
	%	km^2	%	km^2	%	km^2
Obs. point 1: Local DEM – TanDEM-X	82.1	111.8	7.1	9.6	10.9	14.8
Obs. point 1: Local DEM – ALOS PALSAR	82.6	112.5	3.3	4.4	14.1	19.2
Obs. point 1: Local DEM – SRTM	82.5	112.2	1.8	2.5	15.7	21.4
Obs. point 2: Local DEM – TanDEM-X	80.0	109.0	14.4	19.6	5.6	7.6
Obs. point 2: Local DEM – ALOS PALSAR	48.4	65.9	12.7	17.2	39.0	53.1
Obs. point 2: Local DEM – SRTM	47.1	64.0	7.6	10.3	45.4	61.7

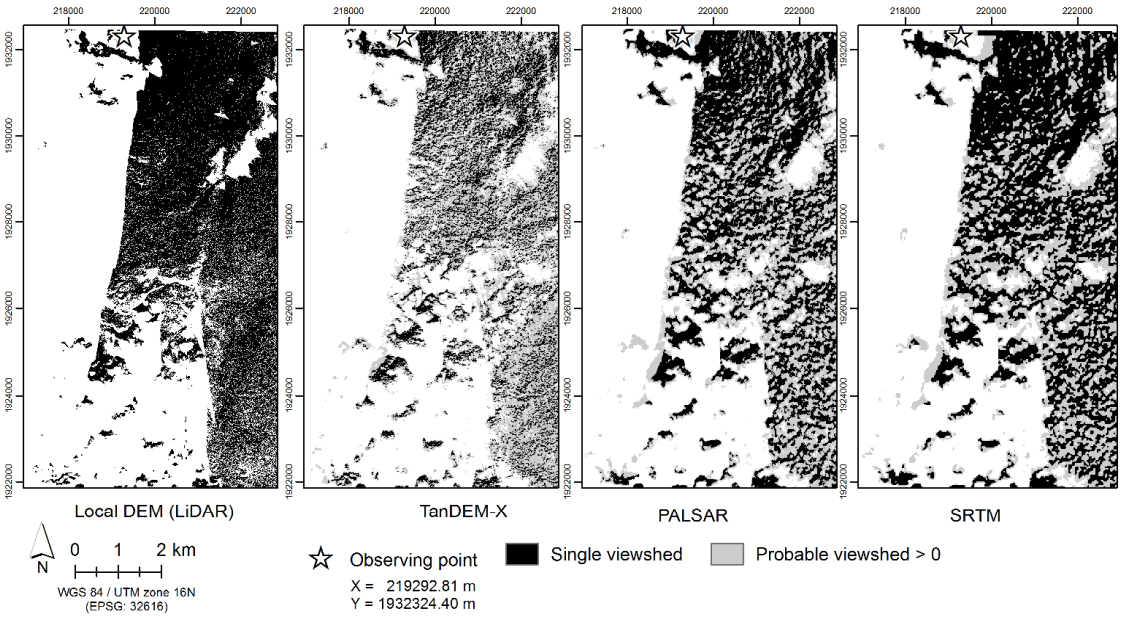

Fig. 4 Observing point 1. From the left: i) the correct single viewshed computed on the local DEM, single viewshed and probable viewshed computed on the ii) TanDEM-X, iii) ALOS PALSAR, iv) SRTM. All cells with the probability higher than 0 are shown.

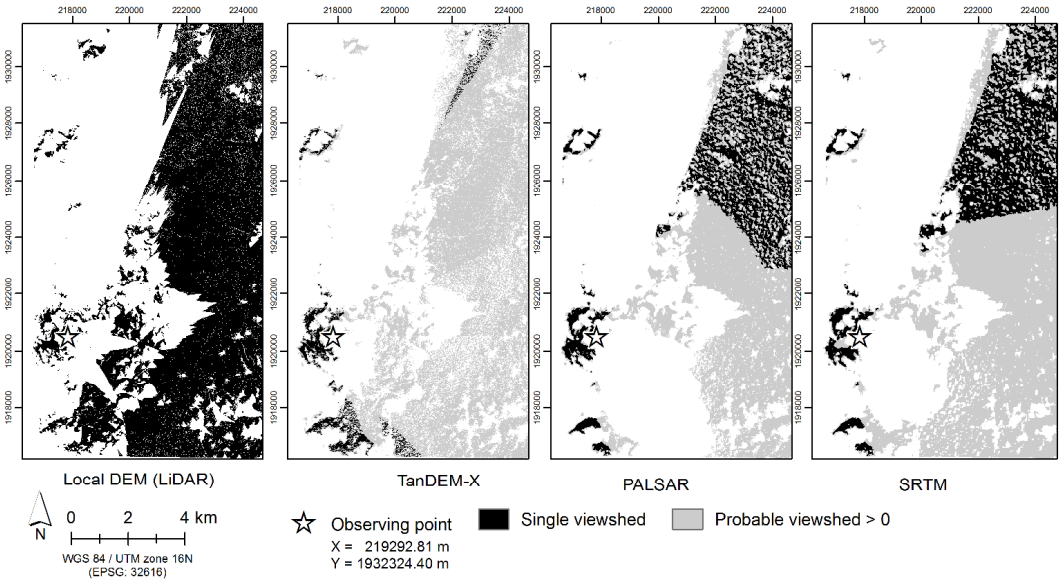

Fig. 5 Observing point 2. From the left: i) the correct single viewshed computed on the local DEM, single viewshed and probable viewshed computed on the ii) TanDEM-X, iii) ALOS PALSAR, iv) SRTM. All cells with the probability higher than 0 are shown.

Conclusions

In this paper, we explored the possibilities of 2.5D modelling of the vegetation, the tree factor, in the visibility analysis. Three cases were examined: i) the opaque vegetation with known extent, ii) the single standing trees that are semitransparent, and iii) opaque vegetation with unknown extent, such as is present in most global DEMs. All presented methods of 2.5D modelling of the vegetation in visibility analysis can be modified and used for different types of obstructions, such as buildings in signal propagation analysis.

Known spatial extent and attributes of the vegetation (height, tree species, density, etc.) allow usage of various modelling techniques (not only those mentioned in this paper). The simplest method is to create a DSM and use it to compute the visibility. When a larger detail is required, high-resolution datasets and 3D modelling may be needed. The semi-transparency, or partial obstruction of the view is mostly relevant when working with the short-distance view with the trees placed near the observer. The level of visibility after the LoS encounters the obstacle can drop continuously or discretely, depending on the specific application.

When the spatial extent of the vegetation is unknown and the analysis is performed using a DEM, where the vegetation is present (or not completely filtered), the probable viewshed may be utilized to estimate the potentially visible areas. In our experiment, we were able to evaluate the results against a more accurate DEM that was sampled at a higher resolution. When the single viewshed computed on the global DEMs was similar to the more accurate local DEM-derived viewshed, the probable viewshed matched the shape of the visible areas. Thus, the result was a more continuous area with less scattered invisible cells. Also, we have observed an interesting behaviour, when the difference between the local and global DEMs was more pronounced. In this case, the probable viewshed correctly identified also those areas that were not visible in the single viewshed.

Thus, this experiment has demonstrated successfully the usage of the probable viewshed to model the potentially visible areas in the landscape, where unwanted vegetation is present in the input DEM. This is crucial for applications that assume different vegetation extents than the current one, e.g., forestry for modelling of the vegetation changes, spatial archaeology with the goal of modelling past landscape, or landscape architecture that is focused on the assessment of the potential visual impact of new structures or other landscape changes.

DMR-3.5 was kindly provided by the Geodetic and Cartographic Institute Bratislava.

Digital elevation model TanDEM-X was kindly provided by the German Aerospace centre DLR as a product of the DLR's TerraSAR-X /TanDEM-X satellite.

Shuttle Radar Topography Mission (SRTM) 1 Arc-Second Global data are available from the U.S. Geological Survey.

ALOS PALSAR (Dataset ALOS PALSAR_Radiometric_Terrain_Corrected_low_res) is a product of Alaska Satellite Facility ASF DAAC 2014; includes Material © JAXA/METI 2007. *DOI: 10.5067/JBYK3J6HFSVF.*

References

CONNOLY, J., LAKE, M. (2006). *Geographical Information Systems in Archaeology*. Cambridge (Cambridge university press).

DEAN, D.J. (1997). Improving the accuracy of forest viewsheds using triangulated networks and the visual permeability method. *Canadian Journal of Forest Research*, 27(7), pp. 969-977.

FELLEMAN, J. (1979). *Landscape Visibility Mapping: Theory and Practice*. New York (School of Landscape Architecture, State University of New York, College of Environmental Science and Forestry).

FISHER, P. (1992). First Experiments in Viewshed Uncertainty: Simulating Fuzzy Viewsheds. *Photogrammetric Engineering & Remote Sensing*, 58(3), pp. 345-352.

LI, X., ZHANG, C., LI, W., KUZOVKINA, Y.A., WEINER, D. (2015). Who lives in greener neighborhoods? The distribution of street greenery and its association with residents' socioeconomic conditions in Hartford, Connecticut, USA. *Urban Forestry and Urban Greening*, 14(4), pp. 751-759.

LIESKOVSKÝ, T., KOVÁČ, M., DRÁPELA, T. (2017). Análisis del uso de LiDAR en el Área de Uaxactun. In Nuevas Excavaciones en Uaxactun VIII. In: *Temporada de Campo 2016*, 2017, Bratislava (Center for Mesoamerican Studies, Comenius University – Chronos), pp. 214-244.

LIN, T., LIN, H., HU, M. (2017). Three-dimensional visibility analysis and visual quality computation for urban open spaces aided by Google SketchUp and WebGIS. *Environment and Planning B: Urban Analytics and City Science*, 44(4), pp. 618-646.

LLOBERA, M. (2007). Modeling visibility through vegetation. *International Journal of Geographic Information Science*, 21(7), pp. 799-810.

MURGOITIO, J., SHRESTHA, R., GLENN, N., SPAETE, L. (2013). Improved visibility calculations with tree trunk obstruction modeling from aerial LiDAR. *International Journal of Geographical Information Science*, 27(10), pp. 1865-1883.

MURGOITIO, J., SHRESTHA, R., GLENN, N., SPAETE, L. (2014). Airborne LiDAR and terrestrial laser scanning derived vegetation obstruction factors for visibility models. *Transactions in GIS*, 18(1), pp.147-160.

NUTSFORD, D., REITSMA, F., PEARSON, A., KINGHAM, S. (2015). Personalising the viewshed: Visibility analysis from the human perspective. *Applied Geography*, 62, pp. 1-7.

RÁŠOVÁ, A. (2014). Fuzzy viewshed , probable viewshed , and their use in the analysis of prehistoric monuments placement in Western Slovakia. In *Connecting a Digital Europe through Location and Place. Proceedings of the AGILE'2014 International Conference on Geographic Information Science, Castellón, June, 3-6, 2014*, pp. 6-8.

RÁŠOVÁ, A. (2018). *Substanciálna analýza viditeľnosti v prostredí GIS*. Dizertačná práca. Bratislava (Slovenská technická univerzita v Bratislave).

WHEATLEY, D., GILLINGS, M. (2000). Vision, perception and GIS: developing enriched approaches to the study of archaeological visibility. In *Beyond the Map, 2000*, Amsterdam, pp. 1-27.

YU, S., YU, B., SONG, W., WU, B., ZHOU, J., HUANG, Y., WU, J., ZHAO, F., MAO, W. (2016). View-based greenery: A three-dimensional assessment of city buildings' green visibility using Floor Green View Index. *Landscape and Urban Planning*, 152, pp.13-26.

R e s u m é

Modelovanie vegetácie v 2,5 analýzach viditeľnosti

Tento článok sa venuje problematike vegetácie v analýzach viditeľnosti, ktoré využívajú 2.5D digitálne výškové modely. Vegetácia je jedným zo substanciálnych faktorov ovplyvňujúcich viditeľnosť a jej modelovanie je náročné kvôli jej premenlivosti v čase a nedostatku spoľahlivých dát vo všeobecnosti.

3D modelovanie vegetácie je stále častejšie využívané v mestských priestoroch, čiže v analýzach viditeľnosti na krátke vzdialenosti, ale tieto postupy nie je možné jednoducho použiť v analýzach na dlhé vzdialenosti kvôli ich komplexnosti a nárokom na dáta s vysokým rozlíšením. V takýchto prípadoch je stále najčastejšie využívané 2D modelovanie. Postupy navrhnuté v tomto článku využívajú bežné 2,5D digitálne výškové modely, takže dosiahnuté výsledky sú jednoducho integrovateľné s ostatnými analytickými vrstvami.

V našich numerických experimentoch sa venujeme trom prípadom: i) nepriehľadnej vegetácii so známym priestorovým umiestnením a známou alebo neznámou výškou, ii) čiastočne priehľadnej vegetácii umiestnenej v blízkosti pozorovacieho bodu, a iii) nepriehľadnej vegetácii s neznámym priestorovým umiestnením.

Najjednoduchší a najčastejšie používaný postup je vytvorenie digitálneho modelu povrchu pridaním vegetácie na digitálny model reliéfu. Ak je výška vegetácie neznáma, ale poznáme jej rozmiestnenie, je možné vypočítať pravdepodobnú viditeľnosť na odhadnutie vplyvu jej výšky.

V prípade samostatne stojacich stromov umiestnených v blízkosti pozorovateľa môže byť potrebné zohľadniť fakt, že nezakrývajú výhľad úplne. Čiastočná priehľadnosť stromov môže byť vyjadrená pomocou koeficientu priepustnosti. Úroveň viditeľnosti po prechode prekážkou môže klesať buď diskrétne alebo kontinuálne, v závislosti od modelovanej situácie.

V najzásadnejšom experimente tohto článku využívame pravdepodobnú viditeľnosť na odhadnutie viditeľnosti neovplyvnenej vegetáciou pri použití globálnych digitálnych výškových modelov. Všetky tri použité modely, SRTM, TanDEM-X a ALOS PALSAR, sú vytvorené radarovou interferometriou, kde je časť vegetácie odfiltrovaná pri spracovaní, avšak jej (neznáma) časť v modeli ostáva. Podarilo sa nám ukázať, že pravdepodobná viditeľnosť vypočítaná s použitím parametrov určených porovnaním s lokálnym digitálnym výškovým modelom s veľmi vysokým rozlíšením, poskytla odhad viditeľnosti, ktorý vystihoval referenčný model výrazne lepšie, než jednoduché viditeľnosti. Tento postup tak môže byť výhodný pri aplikáciách ako je priestorová archeológia či krajinné plánovanie, kde je vegetácia nežiaducim prvkom, avšak nie je ju možné z digitálneho výškového modelu odstrániť.

Obr. 1 Porovnanie viditeľností vypočítaných s použitím (hore, zľava doprava) i) digitálneho modelu reliéfu, ii) digitálneho modelu povrchu, ktorý obsahuje vegetáciu, iii) ich rozdiel a iv) pravdepodobnú viditeľnosť, ktorá zohľadňuje neurčitú výšku vegetácie. Priebeh reliéfu vo výpočtovej oblasti (dole, tieňovaný digitálny model reliéfu DMR-3.5).

Obr. 2 Čiastočne priehľadné prekážky (stromy) s hodnotami koeficientu priepustnosti. Vľavo: diskrétny pokles viditeľnosti, vpravo: spojitý pokles viditeľnosti s použitím exponenciálnej funkcie.

Obr. 3 Výpočtová oblasť v severnej Guatemale (tieňovaný digitálny výškový model TanDEM-X).

Obr. 4 Pozorovací bod 1. Zľava: i) správna jednoduchá viditeľnosť vypočítaná na lokálnom digitálnom výškovom modeli, a jednoduchá a pravdepodobná viditeľnosť vypočítaná na modeloch ii) TanDEM-X, iii) ALOS PALSAR, iv) SRTM. Zobrazené sú všetky bunky s pravdepodobnosťou viditeľnosti vyššou ako 0.

Obr. 5 Pozorovací bod 2. Zľava: i) správna jednoduchá viditeľnosť vypočítaná na lokálnom digitálnom výškovom modeli, a jednoduchá a pravdepodobná viditeľnosť vypočítaná na modeloch ii) TanDEM-X, iii) ALOS PALSAR, iv) SRTM. Zobrazené sú všetky bunky s pravdepodobnosťou viditeľnosti vyššou ako 0.

Tab. 1 Porovnanie oblasti viditeľnej z pozorovacieho bodu 1. Jednoduchá viditeľnosť (SV) nadobúda hodnoty 0 (neviditeľné) alebo 1 (viditeľné). Pravdepodobná viditeľnosť (PV) nadobúda hodnoty z intervalu od 0 po 1.

Tab. 2 Porovnanie oblasti viditeľnej z pozorovacieho bodu 2. Jednoduchá viditeľnosť (SV) nadobúda hodnoty 0 (neviditeľné) alebo 1 (viditeľné). Pravdepodobná viditeľnosť (PV) nadobúda hodnoty z intervalu od 0 po 1.

Tab. 3 Rozdiely medzi pravdepodobnými viditeľnosťami a referenčnou jednoduchou viditeľnosťou vypočítanou z lokálneho digitálneho výškového modelu. Všetky bunky s pravdepodobnosťou viditeľnosti vyššou ako 0 sú považované sa potenciálne viditeľné.

Prijaté do redakcie: 21. júna 2018
Zaradené do tlače: júl 2018